George, S. S., A. K. Wise, J. B. Fallon and R. K. Shepherd (2015). Evaluation of focused multipolar stimulation for cochlear implants in long-term deafened cats. Journal of Neural Engineering 12(3): 036003.

DOI: 10.1088/1741-2560/12/3/036003

Evaluation of focused multipolar stimulation for cochlear implants in long-term deafened cats

Shefin S. George[1,2], **Andrew K. Wise**[1,2], **James B. Fallon**[1,2] **and Robert K. Shepherd**[1,2,*]

[1] The Bionics Institute, East Melbourne, Australia, 3002

[2] Department of Medical Bionics, University of Melbourne, Melbourne, Australia, 3002

Email: rshepherd@bionicsinstitute.org

Abstract

Objective: Focused multipolar (FMP) stimulation has been shown to produce restricted neural activation using intracochlear stimulation in animals with a normal population of spiral ganglion neurons (SGNs). However, in a clinical setting, the widespread loss of SGNs and peripheral fibers following deafness is expected to influence the effectiveness of FMP. *Approach:* We compared the efficacy of FMP stimulation to both monopolar (MP) and tripolar (TP) stimulation in long-term deafened cat cochleae (n=8). Unlike our previous study, these cochleae contained <10% of the normal SGN population adjacent to the electrode array. We also evaluated the effect of electrode position on stimulation modes by using either modiolar facing or lateral wall facing half-band electrodes. The spread of neural activity across the inferior colliculus, a major nucleus within the central auditory pathway, was used as a measure of spatial selectivity. *Main results:* In cochleae with significant SGN degeneration, we observed that FMP and TP stimulation resulted in greater spatial selectivity than MP stimulation (p<0.001). However, thresholds were significantly higher for FMP and TP stimulation compared to MP stimulation (p<0.001). No difference between FMP and TP stimulation was found in any measures. The high threshold levels for FMP stimulation was significantly reduced without compromising spatial selectivity by varying the degree of current focusing (referred as "partial-FMP" stimulation). Spatial selectivity of all stimulation modes was unaffected by the electrode position. Finally, spatial selectivity in long-term deafened cochleae was significantly less than that of cochleae with normal SGN population (George et al., 2014). *Significance:* The present results indicate that the greater spatial selectivity of FMP and TP stimulation over MP stimulation is maintained in cochleae with significant neural degeneration and is not adversely affected by electrode position. The greater spatial selectivity of FMP and TP stimulation would be expected to result in improved clinical performance.

Keywords

Cochlear implant; Current focusing; Electrode configuration; Spatial tuning curve; Inferior colliculus; Deafness

Introduction

Cochlear implants (CIs) electrically stimulate spiral ganglion neurons (SGNs) in order to restore functional hearing in severe-to-profoundly deaf patients. CIs take advantage of the known tonotopic organisation of the inner ear by dividing speech into discrete frequency bands that are mapped to specific electrodes along the electrode array. Conventional CIs typically stimulate the electrodes in a monopolar (MP) configuration, where current is injected between a single intracochlear electrode and a remote extracochlear return electrode. However, the conductive nature of the cochlea leads to spatially broad neural excitation (van den Honert and Stypulkowski, 1987, Bierer and Middlebrooks, 2002); resulting in a limited number of independent stimulation sites (Friesen et al., 2001) and interactions between channels (Bierer and Middlebrooks, 2004, Stickney et al., 2006). While most CI subjects typically receive significant benefit in speech understanding in quiet listening conditions using MP stimulation, their performance diminishes in more difficult listening conditions such as speech in noisy environments and musical perception (Friesen et al., 2001, Shannon et al., 2004). This is likely to be due to limited spatial resolution provided by the implant (Fu et al., 1998, McDermott and McKay, 1997). It is widely anticipated that focusing of stimulation to achieve more spatially restricted patterns of excitation and reduced channel interactions may improve speech and pitch recognition (Nelson et al., 1995, Henry et al., 2000, Bingabr et al., 2008, Srinivasan et al., 2013).

Focused multipolar (FMP) stimulation has been proposed as a method to create focused electrical fields in the cochlea and thus produce a more restricted spread of neural activation compared to conventional MP stimulation. FMP uses multiple independent current sources to simultaneously stimulate all electrodes on the intracochlear electrode array with weighted anodic or cathodic currents in order to restrict or “focus” the electric field. A clinical study conducted on a small group of implant recipients using percutaneous connectors (van den Honert and Kelsall, 2007) has validated FMP stimulation showing that focusing can be achieved, although at the expense of higher stimulation currents required to evoke auditory percepts compared to MP stimulation. This spatial restriction is consistent with the findings of a recent study (Kalkman et al., 2014) which investigated several current focusing paradigms in a computational model of the human cochlea. Psychophysical investigation of FMP stimulation have shown to significantly improve patients ability to discriminate spectral features and dynamic ripple stimuli, suggesting an increase in spectral resolution (Smith et al., 2013). Recently, a clinical study on potential benefits of FMP stimulation for reducing electrode interactions showed a significant reduction in interaction, mainly contributed by electric-field summation, between two spatially separated simultaneous stimuli compared to monopolar stimulation (Marozeau et al., 2015). Consistent with these clinical and modelling studies, we have previously shown that FMP stimulation can produce a narrower spread of activation in the inferior colliculus (IC) compared to MP stimulation in acutely deafened animals, i.e. animals without loss of SGNs or peripheral fibers (George et al., 2014); although again at the expense of an increase in threshold.

Another promising current focusing technique is tripolar (TP) stimulation, where current is delivered to a central intracochlear electrode utilizing two adjacent intracochlear return electrodes. TP stimulation has been reported to produce sharper excitation patterns compared to MP stimulation (Bierer and Middlebrooks, 2002, Snyder et al., 2008, Fielden et al., 2013). However, as with FMP, the increased selectivity comes at the cost of higher current levels to achieve adequate loudness in implant users compared to MP stimulation (Litvak et al., 2007, Berenstein et al., 2008, Landsberger and Srinivasan, 2009). In order to provide greater loudness at the same current level as TP stimuli, partial tripolar (PTP) stimulation has been proposed (Mens and Berenstein, 2005, Litvak et al., 2007, Srinivasan et al., 2013). In PTP, only a portion of current is returned via the adjacent intracochlear electrodes while the remaining current is returned through an extracochlear electrode. Closely analogous to the PTP stimulation, in the present study, we explore the efficacy of a stimulation mode that is referred to here as "partial focused multipolar" or partial-FMP (pFMP) to achieve lower stimulation thresholds compared to the standard focusing FMP stimulation we have used previously (George et al., 2014). The technique involves varying the degree of current focusing by changing the level of compensation current (See Methods section for details).

As outlined above, current focusing techniques typically require high current levels to achieve threshold activation (Bierer and Faulkner, 2010, Zhu et al., 2012). In clinical situations, threshold levels are thought to be influenced by both: a) the pattern of neural survival along the length of the cochlea; and b) the position of the electrode relative to the neural population (Xu et al., 1993, Shepherd et al., 1993, Bierer, 2007, Long et al., 2014). Following sensorineural hearing loss, sensory hair cell loss leads to a number of degenerative and pathological changes to the peripheral processes and the SGNs which are the target neurons of CIs (figure 1). Degeneration is characterized by the retraction of the peripheral processes towards the SGN soma and a more gradual degeneration of the cell bodies within the Rosenthal canal (Nadol et al., 1989, Wise et al., 2005). The degeneration, which is progressive over time, affects SGN responses to an electrical stimulus. Extensive loss of peripheral process and ongoing degeneration of SGNs can result in increased electrical thresholds (Shepherd and Javel, 1997, Landry et al., 2011). An increase in threshold would lead to higher power consumption and result in a greater spread of activation as excitation current spreads within Rosenthal's canal potentially exciting a spatially broad region of SGNs (Frijns et al., 1996).

Another factor that determines the effectiveness of CIs is the radial distance between the electrode and the neural population. There have been several previous studies conducted to investigate the effect of location of the electrode array within the scala tympani on neural excitation. Both electrophysiological (Shepherd et al., 1993, Xu et al., 1993) and psychophysical (Saunders et al., 2002, Long et al., 2014) studies have shown a significant correlation of threshold (electrical/perceptual) current levels with electrode distance from the modiolus. In addition, electrodes in close proximity to SGNs (i.e. adjacent to the modiolar wall), have been shown to produce more restricted neural activation in human cochleae (Cohen et al., 2003) as well as contribute to higher word recognition scores (Holden et al., 2013). It is worth noting that these studies came to a similar conclusion, using a variety of stimulation electrode geometries, that electrodes placed closer to the SGNs are beneficial.

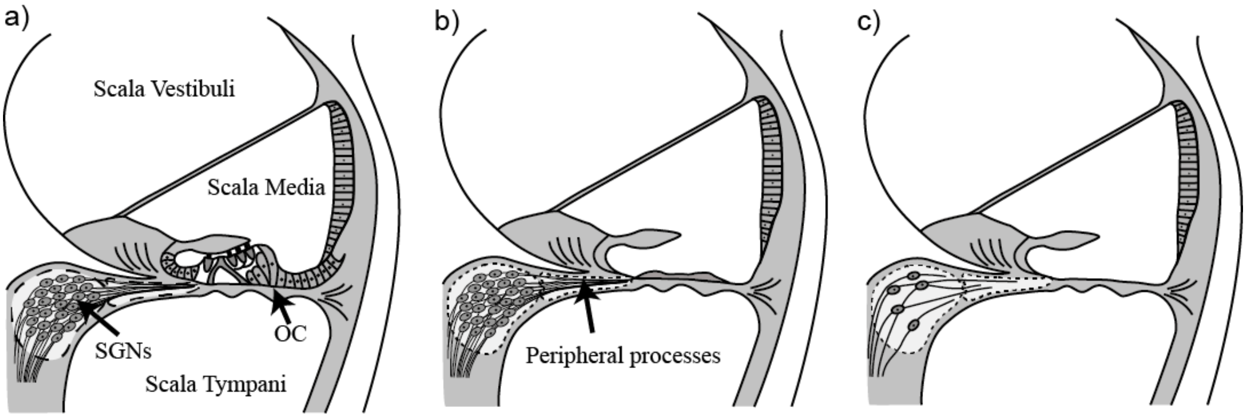

Figure 1: Schematic diagram of a cross-section through a cochlea illustrating the degenerative changes that occur following sensorineural hearing loss (Shepherd et al., 2013). a) Normal cochlea showing the three fluid filled compartments (scala tympani, scala media and scala vestibuli), the organ of Corti (OC) with sensory hair cells and the cell bodies of the spiral ganglion neurons (SGNs) within the Rosenthal's canal. The peripheral process of the SGNs innervate the sensory hair cells b) In a deaf cochlea, the sensory hair cells of the OC is severely damaged which results in the gradual degeneration of the OC. This was the typical status of the SGNs of acutely deafened cochleae in which we conducted our previous study (George et al., 2014) on FMP stimulation (note that the OC would be intact with degenerated sensory hair cells). c) In a long-term deafened cochlea, more gradual degenerative changes such as extensive loss or retraction of peripheral processes and ongoing death of SGNs occur. This is the typical condition of clinically implanted cochleae.

Consequently, in the present study, we examine the efficacy of FMP stimulation compared to MP and TP stimulation in cochleae with significant SGN degeneration, induced by long-term deafness in experimental animals. These data will provide evidence of the efficacy of FMP across clinically relevant populations of SGN survival (Nadol et al., 1989). In addition, pFMP stimulation was investigated to examine the level at which threshold current level can be lowered without compromising spatial selectivity. Finally, we evaluated the influence of electrode position within the scala tympani on spatial selectivity and threshold of FMP stimulation to determine the optimum electrode array placement.

Methods

Experimental animals

Data were collected from six adult cats that were chronically deaf for a duration of 10-12 months. Four animals were implanted unilaterally while two were implanted bilaterally, providing a total of eight implanted cochleae (n=8). Apart from the deafening, the experimental methodology and data analysis reported here are identical to that described in our previous study (George et al., 2014). Therefore, only essential elements of surgical, electrical stimulation and neural recording procedures are outlined here. All procedures were in accordance with the Australian Code of Practice for the Care and Use of Animals for Scientific Purposes and with the National Institutes of Health, USA guidelines regarding the care and use of animals for experimental procedures, and were approved by the Royal Victorian Eye and Ear Hospital Animal Research and Ethics Committee.

Deafening procedure

Each animal was administered a daily injection of neomycin sulfate (60 mg/kg; subcutaneously [s.c]) commencing the day after birth for approximately 20 days (Leake et al., 2000, Fallon et al., 2009). The hearing status of each animal was then measured by recording the auditory brainstem response (ABR) to acoustic stimuli using standard techniques (Coco et al., 2007). If hearing persisted, neomycin injections were continued for three days before the next ABR. This procedure was repeated until the animal was profoundly deaf (i.e. absence of a click-evoked ABR at 100 dB peak equivalent (p.e) sound pressure level (SPL) in both ears).

Physiological data collection

Animals were anaesthetised using ketamine (intramuscular, 20 mg/kg) and xylazil (subcutaneous, 2 mg/kg), and maintained over the duration of the experiment (2-3 days) with a slow continuous intravenous infusion of sodium pentobarbital (3-8 mg/kg/hr). An endotracheal tube was inserted at the beginning of the experiment to monitor respiration rate (normal levels: 10-20) and end-tidal CO_2 levels (normal levels: 3-5%). The core body temperature was maintained at 37.0 ± 1^{o}C.

Animals were implanted with a Hybrid-L 14 array (HL14), consisting of 14 half-band platinum electrodes, inserted approximately 10.5 mm through the round window into the scala tympani (Shepherd et al., 2011). A platinum ball electrode was placed in the neck muscles to serve as the extracochlear return electrode. Following implantation, animals were placed in a stereotaxic frame.

An in-house designed multi-channel stimulator generated all electrical stimuli. Electrical stimuli were cathodic-first, charge balanced single biphasic pulses presented at rate of 4 Hz. The current amplitude was programmed in clinical current level (CL) units defined by Cochlear Corporation, ranging between 0 and 255, where, current in µA = 17.5*(100 ^ (CL/255)). With MP stimulation, current pulses with phase duration of 100 µs and inter-phase gap of 50 µs were delivered to an intracochlear electrode and the extracochlear return electrode. In the TP stimulation configuration, current pulses with 400 µs phase and 50 µs inter-phase gap were delivered to a central intracochlear electrode with two adjacent intracochlear return electrodes, each carrying half the current in opposite phase. In FMP stimulation mode, weighted positive and negative current pulses, with phase durations of either a 100 or 400 µs with a 50 µs inter-phase gap, were delivered simultaneously to multiple electrodes. The differences in pulse durations were a result of the greater charge required using FMP and TP configurations to evoke neural activity. The term “channel” was used to address a set of electrodes used to deliver current in a particular stimulation configuration. The channels were numbered increasing from base to apex, in accordance with the convention used for the clinical CI (figure 2a). The number of its centre electrode indicated each FMP and TP channel. For each FMP channel, the weight vector was constructed based on the strategy adapted from van den Honert and Kelsall (2007). The trans-impedance matrix was measured for all intracochlear electrodes, with each column of the inverse of this matrix used to calculate the numerical weights that determined the current from each electrode to produce a single FMP stimulation channel.

As described in George et al (2014), a craniotomy was performed to expose the entire dorsolateral surface of the contralateral inferior colliculus (IC). Multi-unit recordings to electrical stimulation were made over a range of CLs and different stimulation configurations (MP, FMP and TP). Multi-unit neural activity was recorded using a 32-channel silicon substrate recording array (NeuroNexus Technologies, USA) inserted along the cochleotopic axis of the central nucleus of the IC (figure 2a). The array recorded neural activity over approximately 3.2 mm of the IC. Neural spike activity from the 32 recording sites was amplified, band-pass-filtered (0.3-5 kHz) and digitized at a sample rate of 30 kHz using a Cerebus data acquisition system (Blackrock Microsystems, USA). At the conclusion of the experiment, the animal was euthanized and the cochleae were collected for histological analysis.

Data Analysis

Multi-unit activity was processed offline, using customized spike detection scripts in IgorPro (Wavemetrics, USA). Stimulus artefacts were removed using the techniques detailed in Heffer and Fallon (2008). Spike detection threshold was set at four times root mean square for each recording channel (Fallon et al., 2009). Spikes in a 3-35ms post stimulus window were used in the analysis. The window parameters were based on first-spike latencies and the early onset response of IC neurons to the electrical stimulation (figure 2a). At each recording site, the spike counts were averaged across 10 trials for each stimulus channel, stimulation configuration and current level and normalized to the maximum spike rate.

Response Images

Normalized spike rates (NSRs) recorded across the array were displayed as "response images" with the stimulus intensity on the y-axis and the depth of the recording site on the x-axis (figure 4). Each response image illustrated the spatial extent of evoked multi-unit neural activity across the recording array for a given stimulating channel and stimulus configuration. With each response image, the lowest current level that elicited a NSR of 0.3 was taken as the threshold for that stimulus condition (Landry et al., 2013). The recording site with the lowest threshold was defined as the best recording site.

As the stimulus intensity increased, there was a monotonic increase in neural response. To quantify the growth in neural response with increase in stimulus level at each recording site, the discrimination index, d', was computed using a procedure derived from signal detection theory (Macmillan and Creelman, 2005). The area under the receiver operator curve, formed for each pair of current levels (threshold current level and a supra-threshold current level), was expressed as a standard deviate and the resulting z-score was multiplied by $\sqrt{2}$ to obtain d'.

The value of d' was computed across increasing stimulus levels above the threshold level (i.e NSR = 0.3) for the best recoding site of each stimulating channel. The supra-threshold current level which resulted in a significant increase in the neural response (i.e., the current level that yielded a d' of 1 above the threshold response) was defined as the *distinguishable level* (figure 2c) and this level was chosen to measure spread of activation and total neural response growth in the IC. This distinguishable level was also used to measure the “discrimination slope” of the best recording site (expressed in units of d' per dB; calculated from the difference between the threshold and the distinguishable level) as an indication of dynamic range for the initial slope of the supra-threshold stimulus-response function (Middlebrooks and Snyder, 2007, George et al., 2014). This slope was used as a measure of dynamic range because we seldom saw saturated responses using current focusing techniques within the predefined clinical safety limits of the device.

Effect of SGN degeneration and stimulation configuration on spatial selectivity

To study the effect of SGN degeneration and stimulation configuration on the IC neural response, minimum threshold, discrimination slope, spread of activation and the total neural response growth in the IC were measured for each response image and compared between the MP, FMP and TP stimulation configurations.

a. Spread of activation in the Inferior Colliculus

To quantify the spread of activation, a spatial tuning curve (STC) was constructed for each IC response image by connecting the stimulus levels that elicited threshold response (NSR = 0.3) at each IC recording site (figure 4). The widths of STCs were measured at the distinguishable level and compared between the MP, TP and FMP stimulation configurations.

b. Measure of total neural response growth in the Inferior Colliculus

We measured the total neural response across the recoding array as a correlate for loudness (Litvak et al., 2007, McCreery et al., 2010). We calculated the total neural response for each channel stimulated by summing the NSR on each active recording site at a particular current level. The increases in neural response from threshold level to the distinguishable level were computed and compared across the different stimulus configurations.

Effect of pulse duration on spatial selectivity

With FMP and TP stimulation, high threshold levels and widespread SGN degeneration associated with long-term deafness resulted in requiring longer pulse durations for electrical stimulation. In order to confirm that different pulse durations (100 µs and 400 µs) used in our study did not have a confounding effect on spatial selectivity, sixteen FMP channels with low IC threshold using 400 µs phase duration pulses were also stimulated using 100 µs phase duration. We compared the STC widths and thresholds measured for longer pulses with that of shorter pulses.

Effect of pFMP on spatial selectivity

FMP stimulation involved the measurement of trans-impedances between all electrodes. The trans-impedance matrix was then used to determine current weights for each electrode in such a way that an excitatory voltage was only delivered to the central electrode and null voltage to the other electrodes (van den Honert and Kelsall, 2007). The technique that we have used to vary the degree of focusing was to simply multiply the diagonal terms (calculated by linear extrapolation) of the trans-impedance matrix by a factor called the "Peak Multiplier". Since the effects of the Peak Multiplier were non-linear, we developed a focusing variable called the Defocusing Factor (DF) that varied between 0 and 1, where Peak Multiplier = 1/(1- DF). DF of 0 corresponded to the most focusing or standard FMP stimulation and DF of 1 corresponded to the least focusing or standard MP stimulation (see figure 7 for example). Data was collected from 3 cochleae for this purpose. Twenty-one FMP channels (i.e, channels with at least 2 flanker electrodes on each side) were stimulated at DF of 0.0, 0.1, 0.2, 0.4, 0.6 and 0.8.

Effect of electrode location on spatial selectivity

We implanted two animals bilaterally; in one ear the electrode array was positioned normally (i.e, half band electrodes facing the modiolus) while the electrode array in the other ear was deliberately positioned with the half band electrodes facing the lateral wall (figure 2b). In the remaining four unilaterally implanted animals, the electrode array was positioned normally. This provided a total of 50 channels with the electrode placed normally and 15 channels with the electrode placed in reverse position in order to evaluate the efficacy of stimulation configuration as a function of electrode position within the scala tympani.

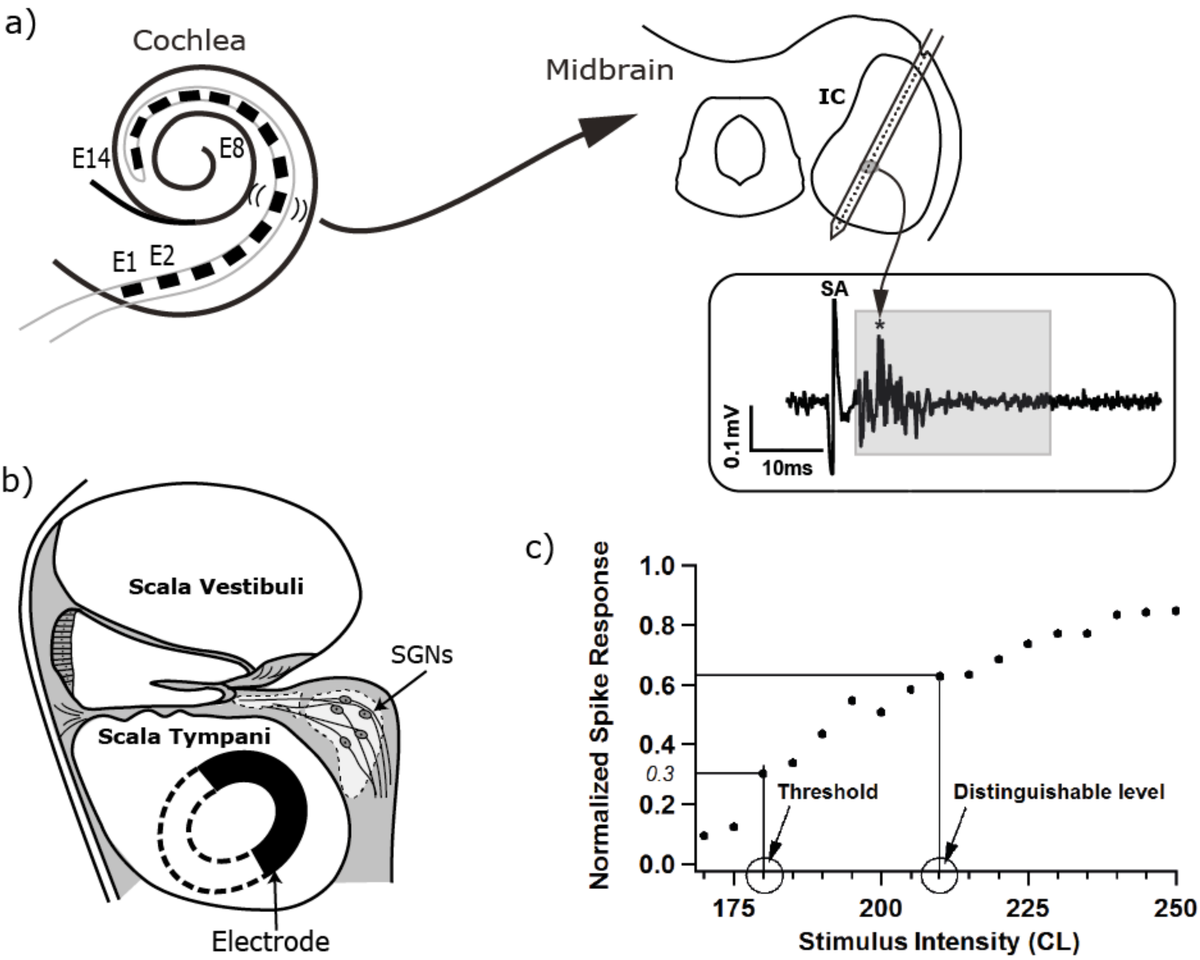

Figure 2: a) Schematic diagram showing an overview of the HL-14 stimulating electrode array implanted into the deafened cochlea and multichannel recording array along the cochleotopic axis of the central nucleus of the contralateral inferior colliculus (IC). The HL-14 electrodes are numbered increasing from base to apex. A trace of multiunit responses (*) and stimulus artefact (SA) from one IC recording site following electrical stimulation is also shown. The analysis window (3-35ms) used for spike counting is shown in the shaded box. **b)** Schematic diagram of a cross-section through a deaf cochlea illustrating the location of the electrode relative to cochlear anatomy. A HL-14 array positioned normally (shaded in black) in the basal turn of scala tympani with the half band electrode

facing the modiolus is shown. This resulted in the electrode being positioned closer to the SGNs compared to the reverse positioning (dashed lines) with the half band electrode facing the lateral wall. **c)** Normalized spike response (NSR) versus stimulus intensity function of the best recording site. The threshold level (i.e., 0.3 NSR) and the distinguishable level (i.e., the current level that resulted in d' of 1 above the threshold response) are indicated in the figure.

Comparison between normal hearing animals and long-term deafened animals

In order to determine whether significant reductions in SGN population will reduce the advantage of FMP stimulation in producing focused neural activation, we compared the STC width and threshold measured for long-term deafened animals with our previous study (George et al., 2014) using acutely deafened animals (i.e, cochleae with normal SGN populations).

Cochlear Histology

To evaluate the extent of SGN degeneration, cochleae of all animals were prepared for histological examination. The implanted cochleae were removed, decalcified, trimmed, embedded in cryosectioning compound and serially sectioned in the modiolar plane at a thickness of 12 µm using a cryostat at -20^{0}C. Sections were stained with haematoxylin and eosin (H&E) and examined under the light microscope. The status of cochlear pathology was determined by measuring the SGN density within the Rosenthal’s canal (Wise et al., 2011). In each section, different cochlear turns (basal, middle and apical) were identified. The area of the Rosenthal’s canal was measured using Carl Zeiss AxioVision LE 4.8.2.0 software and the SGNs in that area with a visible nucleus and nucleoli were counted to determine the density of the SGNs as cells per square millimetres for each cochlear turn.

Statistical Analysis

All statistical analyses were performed using SigmaPlot Version 12.5 (Systat, USA). Comparisons of IC threshold, discrimination slope, STC width and total neural response growth between MP, TP and FMP stimulation were performed using one-way repeated measures ANOVAs, with Tukey corrected post-hoc testing of individual comparisons where appropriate. Comparisons of threshold and STC width measured at 100 µs and 400 µs phase durations with FMP stimulation were performed using a paired *t*-test. Comparisons of threshold and STC width measured for different DFs were performed using one-way repeated measures ANOVAs, with Tukey corrected post-hoc testing of individual comparisons. Comparisons of threshold and STC width measured at two different electrode locations were performed by pooled *t*-test. Where two animal groups (acute and long-term deafened) were compared, a pooled *t*-test was used.

Results

Hearing status and cochlear histology

Following deafening, all the animals had click thresholds ≥ 100 dB p. e. SPL and were therefore confirmed to be profoundly deaf. The cochlear sections were used to examine the status of the organ of Corti and to quantify SGN survival. Figure 3a shows a representative mid-modiolar section illustrating the typical cochlear pathology observed in this study. Analysis of the cochlear histology indicated a total loss of the organ of Corti in all cochlear turns, with reduced SGNs within the Rosenthal's canal and loss of peripheral processes within the osseous spiral lamina. The mean SGN density within the Rosenthal's canal at different cochlear regions measured in this study was compared to the mean SGN density within normal hearing cat cochleae from a previous study (Wise et al., 2011). We observed a significant loss of SGNs in all the cochlear regions (figure 3b), with the basal and middle regions exhibiting around 6-10% SGN survival compared to normal cochleae.

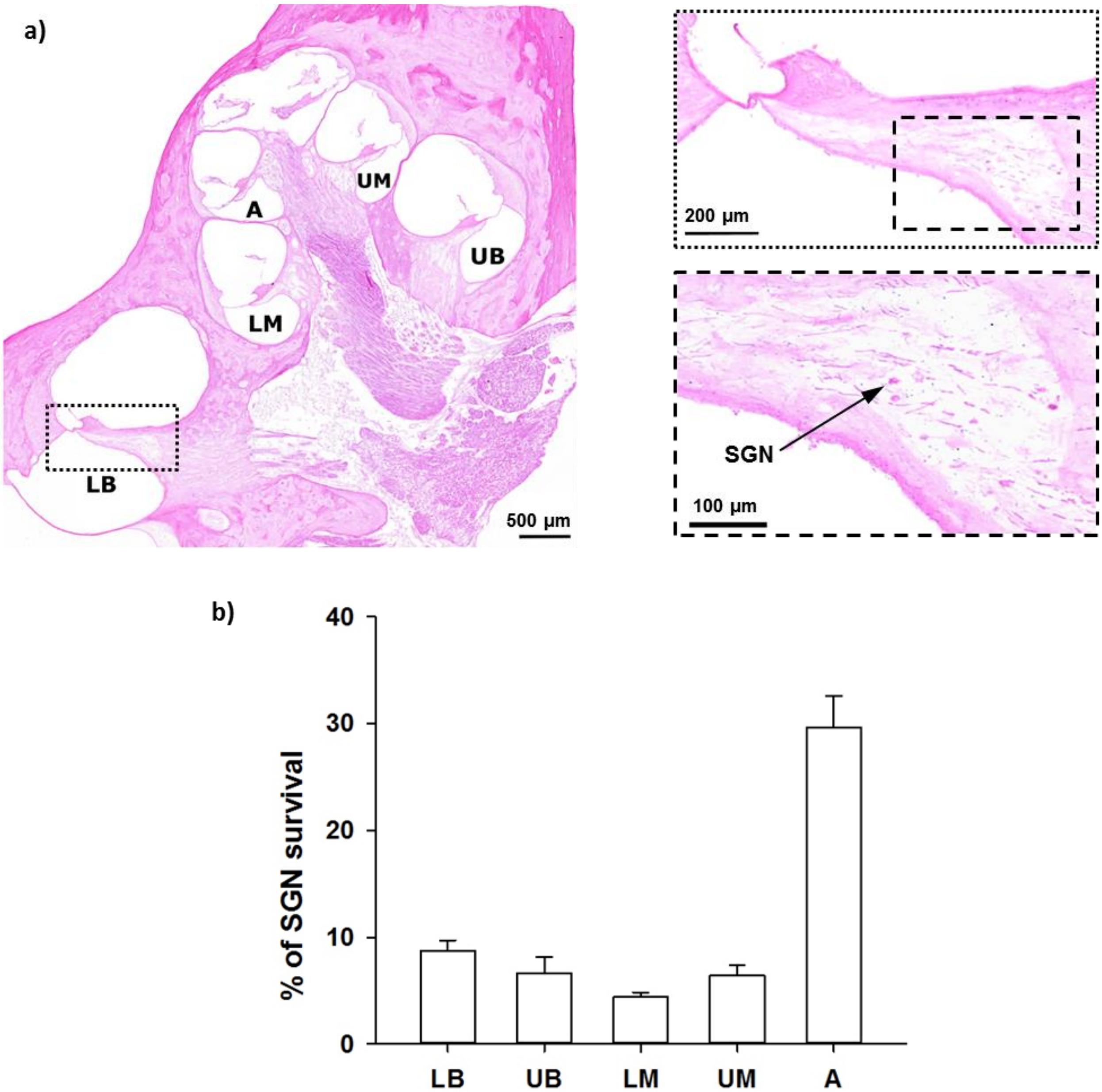

Figure 3 : Photomicrograph of a mid-modiolar section through a long-term deafened cat cochlea a) illustrating the cochlear regions examined i.e. lower basal (LB), upper basal (UB), lower middle (LM), upper middle (UM) and apical (A) regions. The right panels show higher magnification images of lower basal cochlear region illustrating the reduced SGN population. b) Mean % of SGN survival within Rosenthal's canal at different cochlear regions in long-term deafened cochleae (n = 6). Mean SGN density measured in the present study is expressed relative to the data from normal hearing cat cochleae i.e., an average SGN density (expressed in cells per square millimeters) of 1146.1 for LB, 1202.08 for UB, 1289.73 for LM, 1331.36 for UM and 1101.8 for A regions (Wise et al., 2011). Error bar = Standard error of the mean (SEM).

Response Images

IC response images were generated for electrical stimulation with MP, FMP and TP stimulus configurations. Figure 4 presents IC response images from one animal following electrical stimulation of cochlear channel 8 (in the apical sixth of the array) in three different stimulation configurations. In each panel, an STC was plotted by connecting threshold at each IC recording site (shown by the white line). Increases in stimulus intensity above threshold resulted in increasing spread of activation along the recording array and thus, increasing width of the STC. The STCs of FMP and TP stimulation were similarly narrow at low intensities while MP STCs were very broad, generally spreading across the entire recording array and resulting in significant myogenic activity at high intensities (figure 4c).

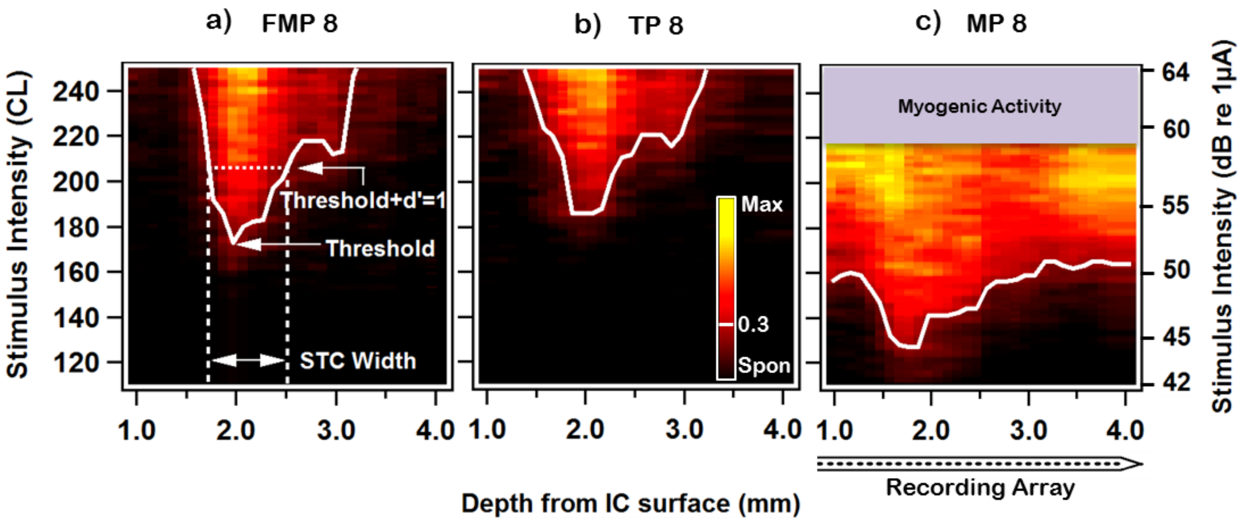

Figure 4: Response images across the cochleotopic axis of the IC to electrical stimulation using a) FMP b) TP and c) MP electrode configurations in a long-term deafened cat. Normalized spike rates (NSR) were represented by colours from yellow to black with yellow representing the highest activity. A spatial tuning curve (STC) was constructed by connecting the stimulus levels that elicited 0.3 NSR on each IC recording site (shown by the white line). The tip of each STC corresponded to the recording site that was most sensitive to that particular electrical stimulus. In this example, the location of the most sensitive recording site corresponded to ~1.9 mm from the IC surface. Each response image was labelled according to configuration and channel number (shown for stimulating channel 8). Note that for MP stimulation, each pulse had a phase of 100 µs while TP and FMP configurations used pulses with 400 µs phase duration, so the differences in electrical threshold between stimulation configurations are not evident in this figure.

Effect of SGN degeneration and electrode configuration on spatial selectivity

Across the six long-term deafened animals, 65 CI channels were stimulated using MP, FMP and TP configurations. Figure 5 shows minimum threshold, discrimination slope, STC width and growth function of the total spike activity for MP, FMP and TP stimulation in long-term deafened cats.

Threshold and discrimination slope

Minimum thresholds, converted to nC per phase, are shown in figure 5a. Mean thresholds were significantly different between stimulation configurations (one-way RM ANOVA, $p < 0.001$); with post-hoc tests indicating that MP stimulation had a significantly lower threshold than FMP or TP stimulation (p's < 0.001) and the thresholds for FMP and TP stimulation were not significantly different ($p = 0.938$). Discrimination slopes for the best recording sites (IC sites with the lowest thresholds) were computed for

MP, FMP and TP stimulation configurations and are presented in figure 5b. There was no significant difference in the discrimination slopes between MP, FMP and TP stimulation configurations (one-way RM ANOVA, $p = 0.827$).

Spread of activation in the inferior colliculus

A repeated measure ANOVA revealed a significant difference among the STC widths measured using different stimulation configurations (figure 5c, $p < 0.001$) and Tukey post hoc analysis confirmed that the STC width was significantly higher for MP than both FMP and TP stimulation configurations (p's < 0.001). There was no significant difference in the STC widths between FMP and TP configurations (p = 0.346).

Measure of total neural response growth in the inferior colliculus

There was a monotonic increase in neural response with increasing stimulus intensity associated with each electrode configuration. The increase in total neural response from the threshold to the distinguishable level was dependent on stimulus configuration (figure 5d; one-way RM ANOVA, $p <$ 0.001) with post-hoc tests confirming that FMP and TP electrode configurations have significantly lower rate of growth compared to the MP configuration ($p < 0.001$). There was no significant difference between FMP and TP configurations ($p = 1$).

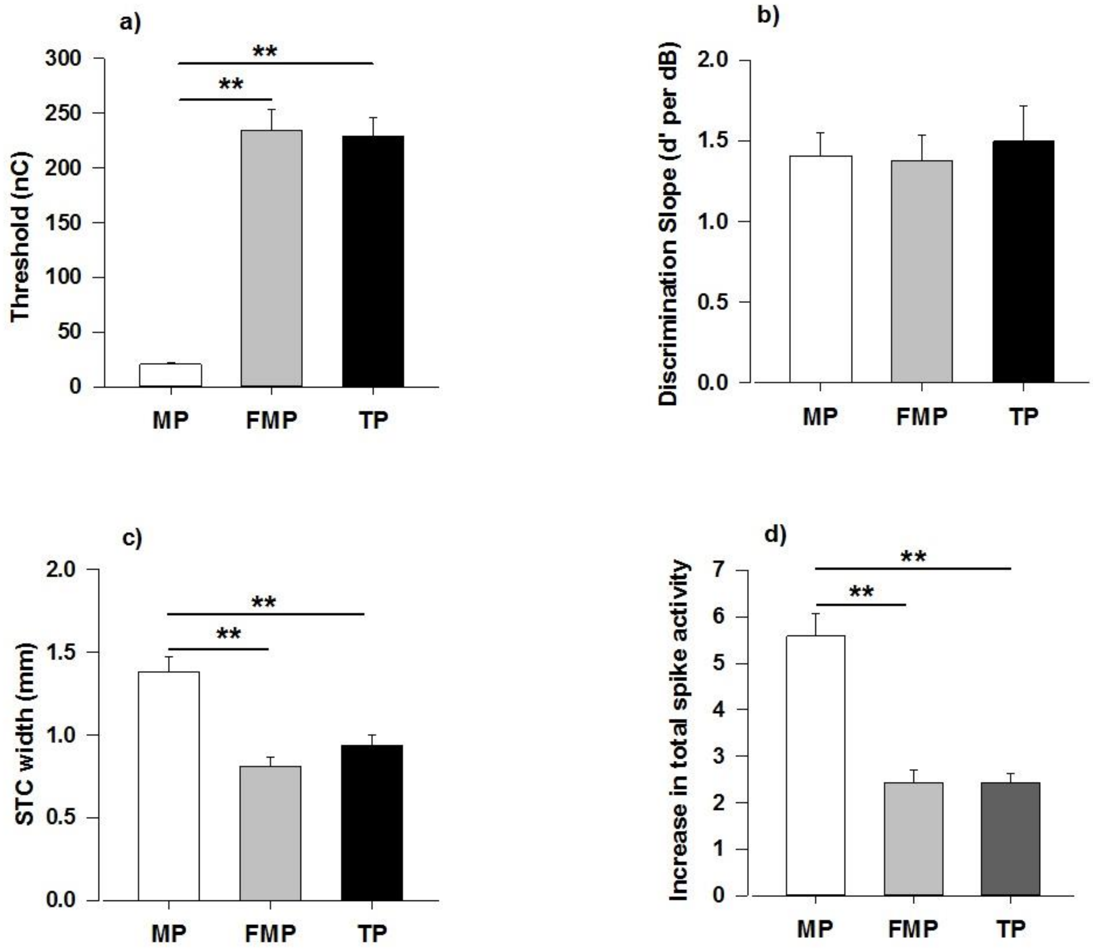

Figure 5: Group means for IC thresholds, discrimination slopes, STC widths and growth function of total spike activity (mean + SEM) measured for MP, FMP and TP stimulation configurations in long-term deafened cats. a)

Threshold levels are expressed in charge (nC). b) Discrimination slope (d' per dB) was calculated from the threshold level and the level that resulted in $d' = 1$ above the threshold level (i.e., the distinguishable level) on the best recording site. c) STC widths (mm) measured at the distinguishable level. d) increase in total spike activity. ** $p < 0.001$, N = 65 channels.

Effect of pulse duration on spatial selectivity

Figure 6 shows the mean threshold and STC width measured for FMP channels stimulated at 100 µs and 400 µs phase duration. As expected, there was a significant difference in the threshold expressed in charge/phase between 100 µs and 400 µs phase duration (figure 6a; paired *t*-test, $p < 0.001$). However, no difference was found between the STC widths (figure 6b; paired *t*-test, $p = 0.625$) at these two pulse durations pooled across 16 FMP channels.

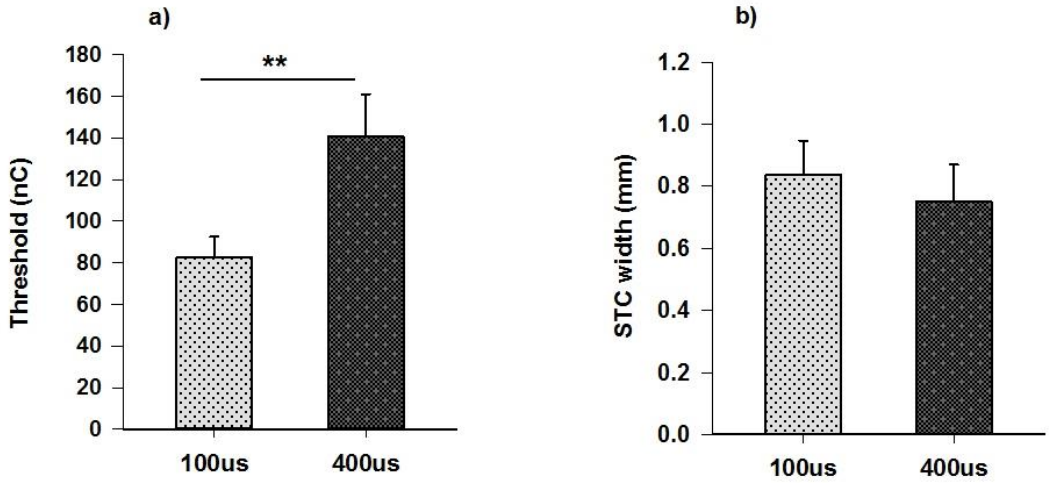

Figure 6: Group means for IC thresholds and STC widths (mean + SEM) measured for FMP stimulation using phase duration of 100 µs and 400 µs in long-term deafened cats. a) Threshold levels expressed in charge (nC). b) STC widths (mm). ** $p < 0.001$, N = 16 channels.

Effect of pFMP stimulation on spatial selectivity

IC response images were plotted for FMP channels at DF of 0, 0.1, 0.2, 0.4, 0.6 and 0.8. Representative response images generated from one animal by stimulating cochlear channel 12 and the corresponding FMP weights on each electrode with DF of 0, 0.2, 0.4 and 0.8 are illustrated in figure 7.

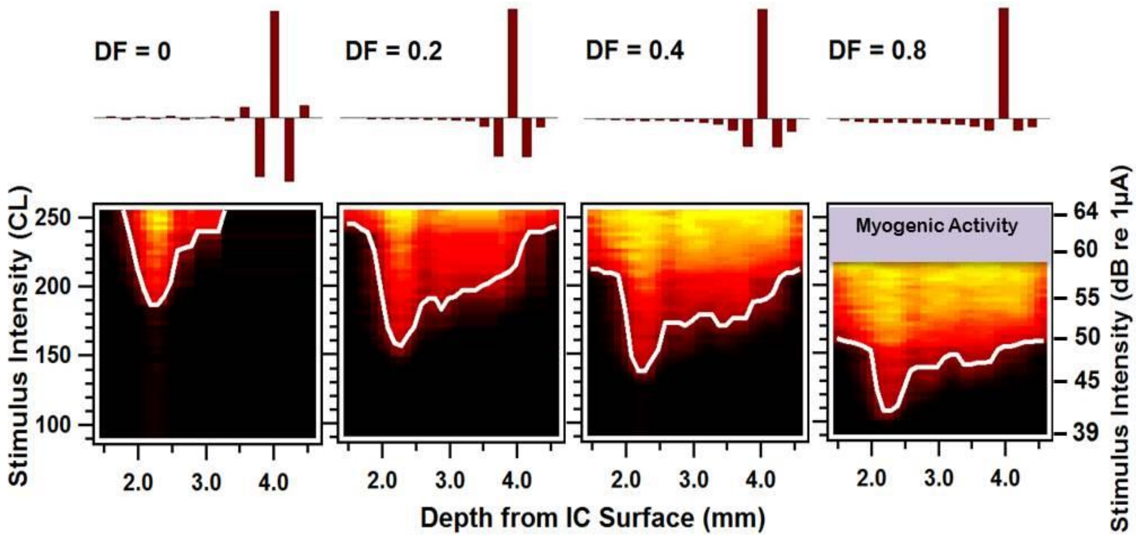

Figure 7: Representative response images across the cochleotopic axis of the IC for pFMP stimulation of cochlear channel 12 using DF of 0.0, 0.2, 0.4 and 0.8. As the DF is increased from 0 to 0.8, the IC threshold (minima of STC) decreased, spread of neural activity increased and the myogenic threshold also decreased. The panel above each response image shows the corresponding weighting of stimulation current for pFMP stimulation of channel 12.

The mean threshold, STC width, discrimination slope and growth rate of total neural spike activity measured with various DFs are shown in figure 8. As expected, the threshold decreased monotonically and the spread of activation increased as DF increased from 0 to 0.8. Threshold at DF of 0 was significantly greater (figure 8a; one-way RM ANOVA) than the threshold at DF of 0.1 ($p < 0.05$), DF of 0.2 ($p < 0.001$), DF of 0.4 ($p < 0.001$), DF of 0.6 ($p < 0.001$) and DF of 0.8 ($p < 0.001$). With STC width, no significant difference was observed on increasing the DF from 0 to 0.6 (figure 8b; one-way RM ANOVA, p's > 0.05) while the widths measured at DF of 0.8 were significantly greater than that measured at DF of 0 ($p < 0.05$). We also performed analyses for STC width measured at a higher supra-threshold level (i.e., the stimulus level that elicited a NSR of 0.7), which exhibited a similar trend as the STC width measured at the distinguishable level (data not shown). One way RM ANOVAs performed on the mean discrimination slopes for different defocusing factors revealed that only the discrimination slope for DF of 0.8 was significantly higher than that for DF of 0 (figure 8c; $p < 0.05$), indicating a reduced dynamic range for the least-focused FMP compared to standard FMP. Moreover, we observed a significant increase in growth rate of total neural response only for DF of 0.8 compared with DF of 0 (figure 8d; one-way RM ANOVA, $p < 0.05$).

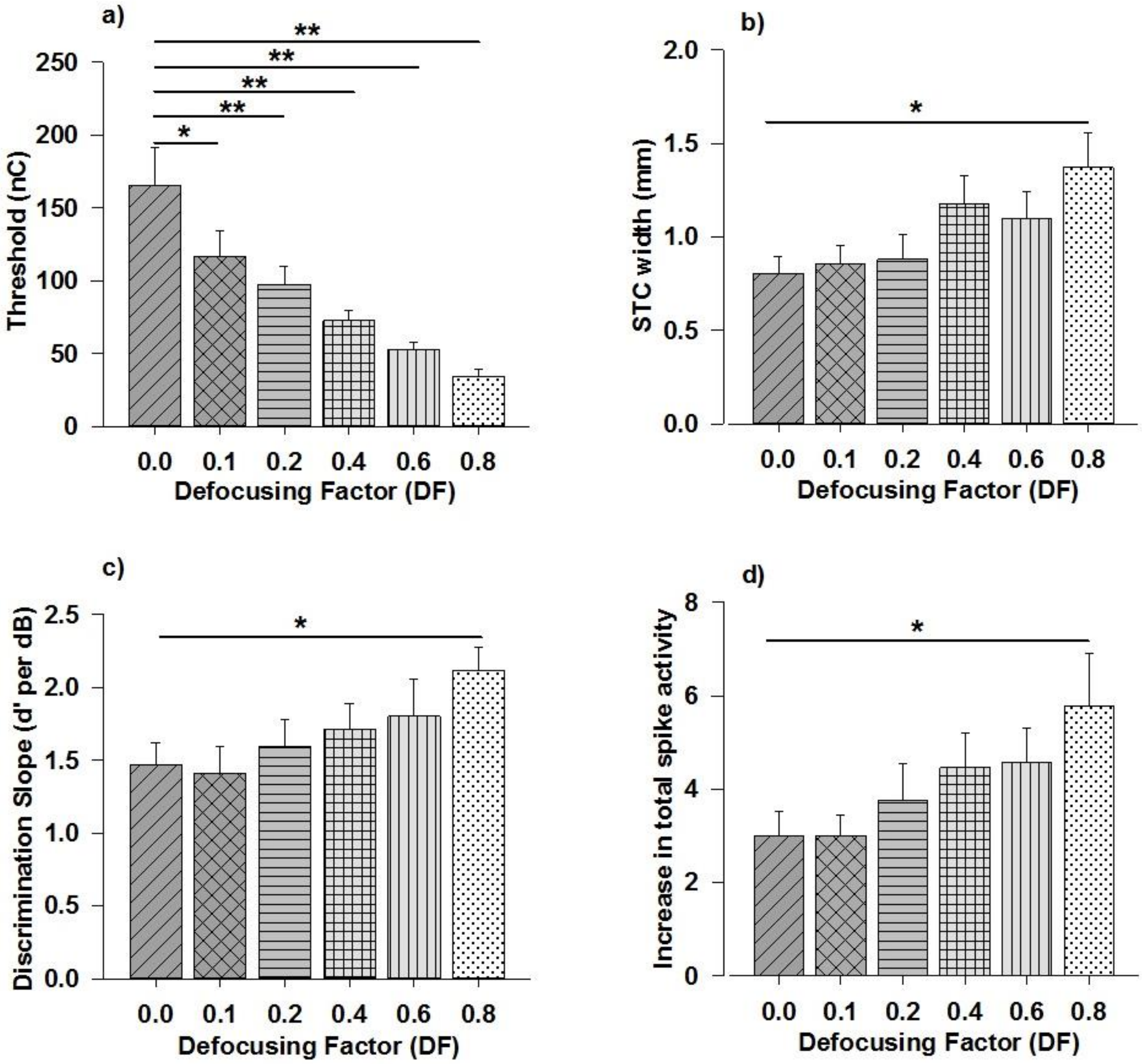

Figure 8: Group means (mean + SEM) for a) Threshold b) STC width c) Discrimination slope and d) Increase in total neural spike activity measured for FMP stimulation with varying defocusing factor (DF) without adjusting the total net current delivered to the intracochlear electrodes. DF of 0 is the most focused stimulus while DF of 0.8 is the least focused. * $p < 0.05$, ** $p < 0.001$, N = 21 channels.

Effect of electrode location on spatial selectivity

Figure 9 shows different features measured to evaluate the efficacy of current focusing with different electrode locations within the cochlea. As expected, there was a small but significant difference in the MP thresholds for the two electrode locations within the scala tympani (figure 9a; *t*-test); thresholds measured with the electrode array in the reverse position were significantly greater than the normal position ($p = 0.002$). However, there was no significant difference in the threshold measured for normal and reverse electrode positioning using FMP (figure 9a; *t*-test, $p = 0.691$) or TP stimulation configurations (*t*-test, $p = 0.782$). No significant difference in the STC width was observed (*t*-test, $p = 0.493$ for MP stimulation, $p = 0.197$ for FMP stimulation and $p = 0.440$ for TP stimulation; figure 9b) for the different electrode array locations.

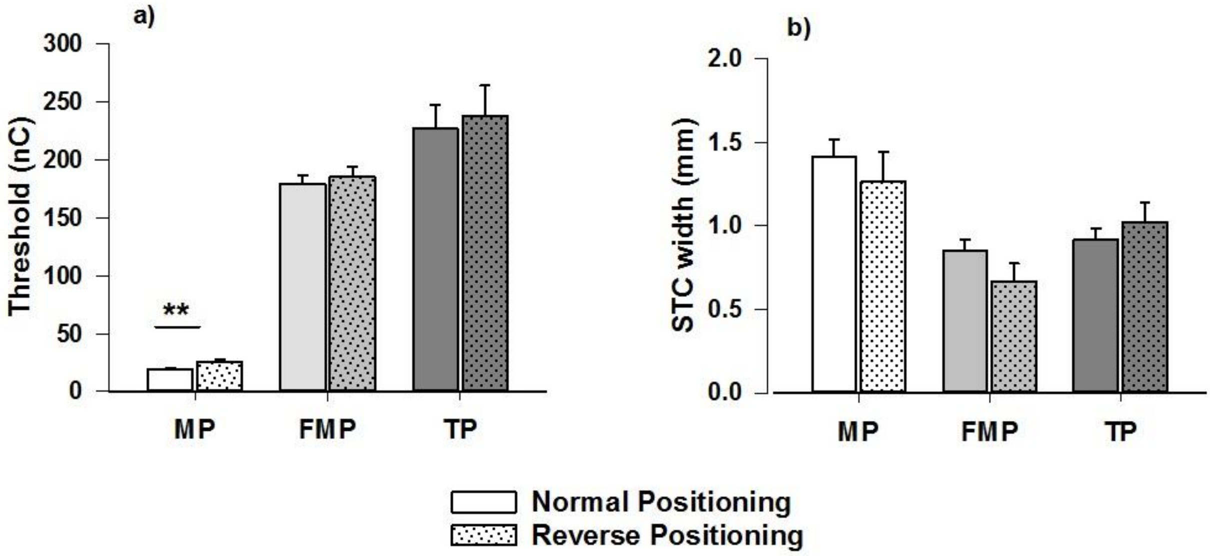

Figure 9: Group means for IC thresholds and STC widths (mean + SEM) measured for MP, FMP and TP stimulation with normal and reverse positioning of the electrode array in long-term deafened cats. a) Threshold levels (nC) b) STC widths (mm). ** $p < 0.001$, N = 50 (Normal position) and 15 (Reverse position) channels.

Comparison between normal hearing animals and long-term deafened animals

Figure 10 show pooled data from acutely deafened cochleae data taken from our previous study (George et al., 2014) in comparison with data from long-term deafened cochleae obtained from the present study. A comparison of IC thresholds from MP stimulation revealed no significant difference between acutely deafened and long-term deafened animals (figure 10a; *t*-test, $p > 0.05$). However, there was a significant difference in FMP and TP thresholds when these two groups were compared; thresholds from long-term deafened cochleae were significantly higher than the acutely deafened cochleae (figure 10a; *t*-test, p's < 0.01). A comparison of STC widths measured for different stimulation configurations revealed a significant difference between the two groups (figure 10b). STC widths obtained from acutely deafened animals were significantly narrower than those from long-term deafened animals (*t*-test, p's < 0.001). There was no significant difference in discrimination slope between the acutely deafened cochleae and the long-term deafened cochleae in any stimulation configuration, indicating that chronic deafness did not affect the dynamic range of each stimulation configuration significantly (figure 10c; *t*-test, p's > 0.05). There was a significant effect of chronic deafness on the growth of total neural response for all stimulation configurations, with rate of growth higher in long-term deafened cochleae compared to acute deafened cochleae (figure 10d; *t*-test, p's < 0.01).

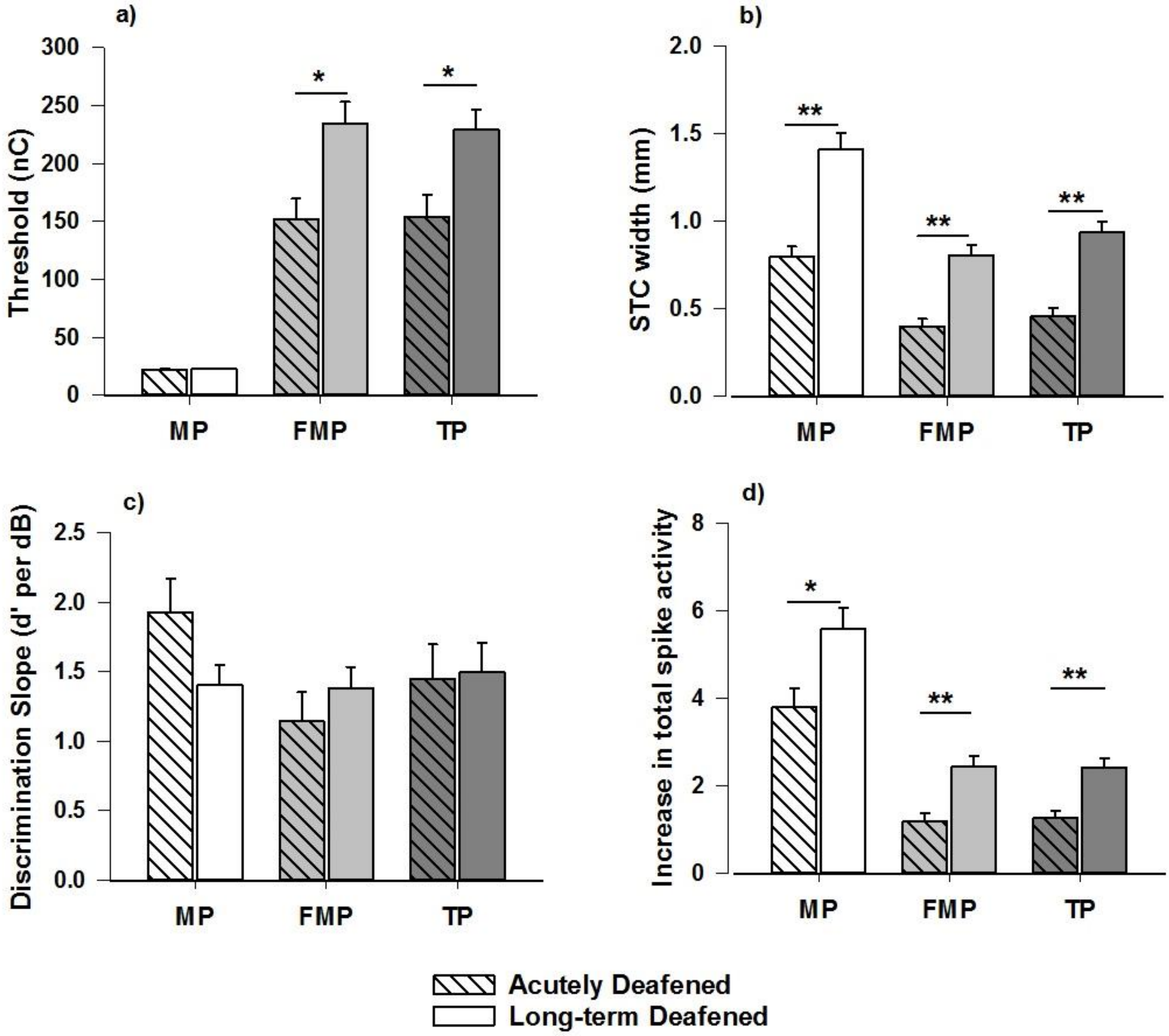

Figure 10: Group means (mean + SEM) for a) IC thresholds (nC), b) STC widths (mm) c) discrimination slope and d) growth function of total spike activity measured for MP, FMP and TP stimulation in acutely deafened cochleae (normal SGN population; from George et al. (2014); N=8) and long-term deafened cochleae (N=8). * $p < 0.01$, ** $p < 0.001$.

Discussion

In the present study, we investigated the effects of SGN degeneration and electrode placement on spatial spread of neural activation using intracochlear FMP stimulation compared to MP and TP stimulation. We also investigated the effects of pulse duration and varying levels of compensation current on spatial selectivity of FMP stimulation.

The main finding of this study was that, in animals with severe SGN degeneration, FMP and TP stimulation produced significantly narrower spatial spread of neural activity in the IC than MP stimulation; although greater current was required to achieve threshold level using FMP and TP stimulation. We found no significant difference in the discrimination slope measured for MP, FMP and TP stimulation, indicating little difference in the dynamic range for different stimulation configurations. In addition, MP stimulation was found to have a rapid growth in total neural response compared to TP and FMP stimulation. However, there was no significant difference between FMP and TP stimulation in any of the measures. In comparison with our previous study (George et al., 2014) that evaluated the efficacy of FMP stimulation in acutely deafened cats with normal SGN survival, the present data from long-term deafened animals demonstrated an elevated IC threshold for FMP and TP stimulation. There was no significant difference in MP threshold between the long-term deafened and acute cochleae, despite the difference in SGN survival. There was a noticeable increase in the width of the STC measured for all the three stimulation configurations in long-term deafened cochleae compared to acute deafened cochleae, suggesting degradation in the stimulation performance with SGN degeneration. However, it should be noted that the spatial extent of neural activation remained significantly smaller with FMP and TP stimulation compared to MP stimulation in long-term deafened cochleae with severe SGN degeneration.

Longer pulse widths were employed with FMP and TP stimulation compared to MP stimulation, as FMP and TP required a greater charge per phase to evoke neural activity than MP. In clinical stimulation strategies, stimulus amplitude and pulse duration are used to modulate the loudness percept. Previous studies have shown that longer pulse durations result in a greater spread of neural activation than stimuli with equal charge/phase or equal loudness using shorter pulse durations (McKay and McDermott, 1999, Shannon, 1985). Consequently, in the present study, it was important to justify the comparison of spread of neural activation produced by FMP stimulation using 400 µs and MP stimulation using 100 µs. Our data indicated that the spatial selectivity of FMP stimulation is not influenced by the phase duration of the electrical stimuli.

Using pFMP stimulation strategy, the present study illustrated a general decrease in the threshold in the IC as the DF was varied from 0 to 0.8. However, there was no significant increase in the STC width on increasing the DF from 0 to 0.6 and a significant increase was observed only on increasing the DF to 0.8. Thus, the present study showed that it is possible to significantly lower the FMP threshold level without a significant increase in the spread of neural activation by raising the DF from 0 up to 0.6. This would be roughly analogous to partial tripolar (pTP), a configuration similar to TP (Kral et al., 1998, Litvak et al., 2007, Landsberger et al., 2012). This configuration has been shown to provide the benefits of both TP and MP stimulation by preserving restricted neural activation while lowering the threshold current level (Mens and Berenstein, 2005, Srinivasan et al., 2013). The present study also showed a gradual increase in the discrimination slope of the best recording site on moving from the standard FMP (DF=0) to the least-focused FMP (DF=0.8) with a significant difference observed between DF of 0 and 0.8. This indicates a reduced dynamic range for the less-focused FMP, at least for the initial slope of the supra-threshold stimulus-response function. Even though our analysis focused on the responses at a near-threshold level, we observed a similar trend with the spread of activation when measured at a higher stimulus level (i.e., at the level that elicited a NSR of 0.7).

In the present study, we observed significant increases in MP threshold levels when the electrode array was implanted in the reverse position. This observation is consistent with a number of previous studies that reported that an electrode array placed closer to the modiolar wall results in lower threshold levels (Xu et al., 1993, Shepherd et al., 1993, Saunders et al., 2002). However, in a somewhat surprising result, we observed that the position of the electrode array did not appear to affect FMP and TP threshold levels. Additionally, the spatial selectivity during MP, FMP and TP stimulation was unaffected by electrode position. This suggests that the efficacy of current focusing techniques to produce restricted neural activation is not compromised with electrode position within the scala tympani. This is in contrast to a clinical study (Cohen et al., 2003) in which the effect of electrode type on the spatial extent of electrically evoked compound action potential (ECAP), estimating the peripheral spread of neural excitation, was investigated using MP stimulation. The mean width was found to be significantly smaller for the half-banded modiolar hugging Contour array compared to a straight banded array, indicating a positive correlation between the spread of neural excitation and the radial distance of the electrode from the modiolus. The discrepancy between the results of the present study and the Cohen et al. study is likely to be related to a number of factors. Firstly, the different distances between the electrode and the target SGNs; the two electrode positions (normal and reverse) tested in the present study would have resulted in less variation in the radial distance of the electrode from the modiolus than in the Cohen et al. study. Secondly, the change in selectively observed by Cohen et al. may also have resulted from changes in the geometry of the electrode (half-band compared to full-band). Thirdly, it is likely that the ECAP results of Cohen et al. are influenced by the effect of electrode position on recordings as well as any effect on the stimulation itself. Finally, Saunders et al. (2002) has suggested that several factors such as the etiology of the hearing loss and pattern of fibrous tissue growth can influence the correlation between the psychophysical measures and electrode distance, so it is worth noting that all electrodes were acutely implanted in the current study, so there would have been no fibrous tissue capsule.

In the present study, the results indicate that current focusing is not highly dependent on distance from the SGNs, at least within the confines of the dimensions of the cat cochlea. In a recent modelling study, Kalkman et al. (2014) showed that current focusing using FMP was not diminished using electrodes positioned along the lateral wall of the cochlea. Indeed, Kalkman demonstrated improved focusing using this electrode position compared to electrodes placed close to the SGNs. The finding that spatial selectivity for all stimulation modes was unaffected by the electrode position could be interpreted as the site of stimulation in these experiments had spread centrally to the auditory nerve or the auditory brainstem. However, we observed a systemic shift in the location of the most sensitive IC recording site to more ventromedial locations when moving the electrical stimuli from an apical cochlear channel to a more basal channel, consistent with the fact that were selectively stimulating SGNs within the cochlea.

In short, the present study has indicated that the high degree of spatial selectivity achieved using FMP stimulation compared to MP stimulation is maintained in cochleae with low SGN survival and in situations when the electrodes are positioned proximal to the lateral wall. Moreover, the spatial selectivity measures of FMP stimulation remained unchanged across phase durations of 100-400 µs. The study also illustrates how threshold level can systematically decrease as the degree of “focusing” is varied from the most focused (DF=0) to the least focused (DF=0.8). Importantly, on comparing long-term deafened cochleae with cochleae having normal SGN and peripheral fiber populations, we saw a significant increase in STC width for MP, FMP and TP stimulation and a significant increase in FMP and TP thresholds.

Clinical Significance

The difference in SGN survival patterns across different listeners is likely to contribute to the variability in CI performance from listener to listener. Recently, Seyyedi et al. (2014) reported a positive correlation between speech perception scores using conventional stimulation strategies and overall SGN count. Technologies designed to improve the electrode-neural interface may be important in optimizing the effectiveness of new stimulation strategies for improved CI performance. In the present study, the performance of current focusing techniques was associated with the SGN survival. Significantly higher stimulation currents were required to achieve threshold activation in cochleae with extensive SGN loss. Biological interventions aimed at preserving SGNs and their peripheral process and promoting their regrowth, such as the administration of exogenous neurotrophins (Wise et al., 2012), may play an important role in concert with current focusing techniques in enhancing CI function.

Importantly, FMP stimulation has the potential to provide benefit for other neural prostheses such as deep brain stimulation to treat movement disorders and spinal cord stimulation to manage chronic pain, where excitation of non-target neurones could cause adverse side effects. Techniques that effectively focus electrical stimulation will provide a benefit for these systems by ensuring a more precise and controlled form of neural activation.

We have shown that FMP stimulation produces highly spatially restricted excitation in cochleae with normal and severe SGN loss. Future experimental work is required to investigate whether FMP stimulation can increase the number of temporally independent channels and to examine the long-term safety of FMP stimulation.

Acknowledgements

This study was funded by The Garnett Passe and Rodney Williams Memorial Foundation, the ARC (LP 130 100 220) and the NHMRC. SSG was supported by an Australian Postgraduate Award through the Australian Government and the Bartholomew Reardon PhD Scholarship through the Bionics Institute. The Bionics Institute acknowledges the support it receives from the Victorian Government through its Operational Infrastructure Support Program. We thank Dr. Zachary Smith and Dr. Christopher Long for experimental protocol contributions, Philipp Senn for multi-channel stimulator engineering and support, Dr. Dexter Irvine and Sam Irving for surgical assistance, Helen Feng for electrode manufacture, Nicole Critch for animal care and Dr. Sue Pierce for veterinary advice.

Reference

BERENSTEIN, C. K., MENS, L. H., MULDER, J. J. & VANPOUCKE, F. J. 2008. Current steering and current focusing in cochlear implants: comparison of monopolar, tripolar, and virtual channel electrode configurations. *Ear Hear,* 29**,** 250-60.

BIERER, J. A. 2007. Threshold and channel interaction in cochlear implant users: evaluation of the tripolar electrode configuration. *J. Acoust. Soc. Am,* 121**,** 1642-53.

BIERER, J. A. & FAULKNER, K. F. 2010. Identifying cochlear implant channels with poor electrode-neuron interface: partial tripolar, single-channel thresholds and psychophysical tuning curves. *Ear and hearing,* 31**,** 247.

BIERER, J. A. & MIDDLEBROOKS, J. C. 2002. Auditory cortical images of cochlear-implant stimuli: dependence on electrode configuration. *J Neurophysiol,* 87**,** 478-92.

BIERER, J. A. & MIDDLEBROOKS, J. C. 2004. Cortical responses to cochlear implant stimulation: channel interactions. *J. Assoc. Res,* 5**,** 32-48.

BINGABR, M., ESPINOZA-VARAS, B. & LOIZOU, P. C. 2008. Simulating the effect of spread of excitation in cochlear implants. *Hear. Res,* 241**,** 73-9.

COCO, A., EPP, S. B., FALLON, J. B., XU, J., MILLARD, R. E. & SHEPHERD, R. K. 2007. Does cochlear implantation and electrical stimulation affect residual hair cells and spiral ganglion neurons? *Hear. Res,* 225**,** 60-70.

COHEN, L. T., RICHARDSON, L. M., SAUNDERS, E. & COWAN, R. S. 2003. Spatial spread of neural excitation in cochlear implant recipients: comparison of improved ECAP method and psychophysical forward masking. *Hearing research,* 179**,** 72-87.

FALLON, J. B., IRVINE, D. R. & SHEPHERD, R. K. 2009. Cochlear implant use following neonatal deafness influences the cochleotopic organization of the primary auditory cortex in cats. *J. Comp. Neurol,* 512**,** 101-14.

FIELDEN, C. A., KLUK, K. & MCKAY, C. M. 2013. Place specificity of monopolar and tripolar stimuli in cochlear implants: The influence of residual masking. *J. Acoust. Soc. Am,* 133**,** 4109-23.

FRIESEN, L. M., SHANNON, R. V., BASKENT, D. & WANG, X. 2001. Speech recognition in noise as a function of the number of spectral channels: comparison of acoustic hearing and cochlear implants. *J. Acoust. Soc. Am,* 110**,** 1150-63.

FRIJNS, J., DE SNOO, S. & TEN KATE, J. 1996. Spatial selectivity in a rotationally symmetric model of the electrically stimulated cochlea. *Hearing research,* 95**,** 33-48.

FU, Q. J., SHANNON, R. V. & WANG, X. 1998. Effects of noise and spectral resolution on vowel and consonant recognition: acoustic and electric hearing. *J. Acoust. Soc. Am,* 104**,** 3586-96.

GEORGE, S. S., WISE, A. K., SHIVDASANI, M. N., SHEPHERD, R. K. & FALLON, J. B. 2014. Evaluation of focused multipolar stimulation for cochlear implants in acutely deafened cats. *Journal of neural engineering,* 11**,** 065003.

HEFFER, L. F. & FALLON, J. B. 2008. A novel stimulus artifact removal technique for high-rate electrical stimulation. *Journal of neuroscience methods,* 170**,** 277-284.

HENRY, B. A., MCKAY, C. M., MCDERMOTT, H. J. & CLARK, G. M. 2000. The relationship between speech perception and electrode discrimination in cochlear implantees. *J. Acoust. Soc. Am,* 108**,** 1269-80.

HOLDEN, L. K., FINLEY, C. C., FIRSZT, J. B., HOLDEN, T. A., BRENNER, C., POTTS, L. G., GOTTER, B. D., VANDERHOOF, S. S., MISPAGEL, K. & HEYDEBRAND, G. 2013. Factors affecting open-set word recognition in adults with cochlear implants. *Ear and hearing,* 34**,** 342.

KALKMAN, R. K., BRIAIRE, J. J. & FRIJNS, J. H. 2014. Current focusing in cochlear implants: An analysis of neural recruitment in a computational model. *Hearing research,* http://dx.doi.org/10.1016/j.heares.2014.12.004.

KRAL, A., HARTMANN, R., MORTAZAVI, D. & KLINKE, R. 1998. Spatial resolution of cochlear implants: the electrical field and excitation of auditory afferents. *Hear. Res,* 121**,** 11-28.

LANDRY, T. G., FALLON, J. B., WISE, A. K. & SHEPHERD, R. K. 2013. Chronic neurotrophin delivery promotes ectopic neurite growth from the spiral ganglion of deafened cochleae without compromising the spatial selectivity of cochlear implants. *J. Comp. Neurol,* 521**,** 2818-32.

LANDRY, T. G., WISE, A. K., FALLON, J. B. & SHEPHERD, R. K. 2011. Spiral ganglion neuron survival and function in the deafened cochlea following chronic neurotrophic treatment. *Hear. Res,* 282**,** 303-13.

LANDSBERGER, D. M., PADILLA, M. & SRINIVASAN, A. G. 2012. Reducing current spread using current focusing in cochlear implant users. *Hear. Res,* 284**,** 16-24.

LANDSBERGER, D. M. & SRINIVASAN, A. G. 2009. Virtual channel discrimination is improved by current focusing in cochlear implant recipients. *Hear. Res,* 254**,** 34-41.

LEAKE, P. A., SNYDER, R. L., REBSCHER, S. J., MOORE, C. M. & VOLLMER, M. 2000. Plasticity in central representations in the inferior colliculus induced by chronic single- vs. two-channel electrical stimulation by a cochlear implant after neonatal deafness. *Hear. Res,* 147**,** 221-41.

LITVAK, L. M., SPAHR, A. J. & EMADI, G. 2007. Loudness growth observed under partially tripolar stimulation: model and data from cochlear implant listeners. *J. Acoust. Soc. Am,* 122**,** 967-81.

LONG, C. J., HOLDEN, T. A., MCCLELLAND, G. H., PARKINSON, W. S., SHELTON, C., KELSALL, D. C. & SMITH, Z. M. 2014. Examining the Electro-Neural Interface of Cochlear Implant Users Using Psychophysics, CT Scans, and Speech Understanding. *J. Assoc. Res,* 15**,** 293-304.

MACMILLAN, N. A. & CREELMAN, C. D. 2005. *Detection theory: A user's guide,* New Jersy, Lawrence Erlbaum.

MAROZEAU, J., MCDERMOTT, H. J., SWANSON, B. A. & MCKAY, C. M. 2015. Perceptual interactions between electrodes using focused and monopolar cochlear stimulation. *J. Assoc. Res. Otolaryngol,* in press.

MCCREERY, D., HAN, M. & PIKOV, V. 2010. Neuronal activity evoked in the inferior colliculus of the cat by surface macroelectrodes and penetrating microelectrodes implanted in the cochlear nucleus. *IEEE Trans. Biomed. Eng,* 57**,** 1765-73.

MCDERMOTT, H. J. & MCKAY, C. M. 1997. Musical pitch perception with electrical stimulation of the cochlea. *J. Acoust. Soc. Am,* 101**,** 1622-31.

MCKAY, C. M. & MCDERMOTT, H. J. 1999. The perceptual effects of current pulse duration in electrical stimulation of the auditory nerve. *J. Acoust. Soc. Am,* 106**,** 998-1009.

MENS, L. H. & BERENSTEIN, C. K. 2005. Speech perception with mono- and quadrupolar electrode configurations: a crossover study. *Otology & neurotology : official publication of the American Otological Society, American Neurotology Society [and] European Academy of Otology and Neurotology,* 26**,** 957-64.

MIDDLEBROOKS, J. C. & SNYDER, R. L. 2007. Auditory prosthesis with a penetrating nerve array. *J. Assoc. Res,* 8**,** 258-79.

NADOL, J., YOUNG, Y. & GLYNN, R. 1989. Survival of spiral ganglion cells in profound sensorineural hearing loss: implications for cochlear implantation. *The Annals of otology, rhinology, and laryngology,* 98**,** 411-16.

NELSON, D. A., VAN TASELL, D. J., SCHRODER, A. C., SOLI, S. & LEVINE, S. 1995. Electrode ranking of ‘‘place pitch’’and speech recognition in electrical hearing. *J. Acoust. Soc. Am,* 98**,** 1987-99.

SAUNDERS, E., COHEN, L., ASCHENDORFF, A., SHAPIRO, W., KNIGHT, M., STECKER, M., RICHTER, B., WALTZMAN, S., TYKOCINSKI, M. & ROLAND, T. 2002. Threshold, comfortable level and impedance changes as a function of electrode-modiolar distance. *Ear Hear,* 23**,** 28S-40S.

SEYYEDI, M., VIANA, L. M. & NADOL JR, J. B. 2014. Within-Subject Comparison of Word Recognition and Spiral Ganglion Cell Count in Bilateral Cochlear Implant Recipients. *Otology & neurotology: official publication of the American Otological Society, American Neurotology Society [and] European Academy of Otology and Neurotology*.

SHANNON, R. V. 1985. Threshold and loudness functions for pulsatile stimulation of cochlear implants. *Hear. Res,* 18**,** 135-43.

SHANNON, R. V., FU, Q.-J. & GALVIN 3RD, J. 2004. The number of spectral channels required for speech recognition depends on the difficulty of the listening situation. *Acta oto-laryngologica. Supplementum,* 552**,** 50-54.

SHEPHERD, R., HATSUSHIKA, S. & CLARK, G. M. 1993. Electrical stimulation of the auditory nerve: the effect of electrode position on neural excitation. *Hear. Res,* 66**,** 108-20.

SHEPHERD, R., VERHOEVEN, K., XU, J., RISI, F., FALLON, J. & WISE, A. 2011. An improved cochlear implant electrode array for use in experimental studies. *Hear. Res,* 277**,** 20-27.

SHEPHERD, R., WISE, A. & FALLON, J. 2013. Chapter 16 - Cochlear implants. *In:* GASTONE, G. C. (ed.) *Handbook of Clinical Neurophysiology.* Elsevier.

SHEPHERD, R. K. & JAVEL, E. 1997. Electrical stimulation of the auditory nerve. I. Correlation of physiological responses with cochlear status. *Hear. Res,* 108**,** 112-44.

SMITH, Z. M., PARKINSON, W. S. & LONG, C. J. Multipolar current focusing increases spectral resolution in cochlear implants. Engineering in Medicine and Biology Society (EMBC), 2013 35th Annual International Conference of the IEEE, 2013. IEEE, 2796-99.

SNYDER, R. L., MIDDLEBROOKS, J. C. & BONHAM, B. H. 2008. Cochlear implant electrode configuration effects on activation threshold and tonotopic selectivity. *Hear. Res,* 235**,** 23-38.

SRINIVASAN, A. G., PADILLA, M., SHANNON, R. V. & LANDSBERGER, D. M. 2013. Improving speech perception in noise with current focusing in cochlear implant users. *Hearing research,* 299**,** 29-36.

STICKNEY, G. S., LOIZOU, P. C., MISHRA, L. N., ASSMANN, P. F., SHANNON, R. V. & OPIE, J. M. 2006. Effects of electrode design and configuration on channel interactions. *Hear. Res,* 211**,** 33-45.

VAN DEN HONERT, C. & KELSALL, D. C. 2007. Focused intracochlear electric stimulation with phased array channels. *J Acoust Soc Am,* 121**,** 3703-16.

VAN DEN HONERT, C. & STYPULKOWSKI, P. H. 1987. Single fiber mapping of spatial excitation patterns in the electrically stimulated auditory nerve. *Hear. Res,* 29**,** 195-206.

WISE, A., WISE, L. & GILLESPIE 2012. Drug delivery to the inner ear. *Journal of neural engineering,* 9**,** 065002.

WISE, A. K., FALLON, J. B., NEIL, A. J., PETTINGILL, L. N., GEANEY, M. S., SKINNER, S. J. & SHEPHERD, R. K. 2011. Combining cell-based therapies and neural prostheses to promote neural survival. *Neurotherapeutics,* 8**,** 774-787.

WISE, A. K., RICHARDSON, R., HARDMAN, J., CLARK, G. & O'LEARY, S. 2005. Resprouting and survival of guinea pig cochlear neurons in response to the administration of the neurotrophins brain-derived neurotrophic factor and neurotrophin-3. *J. Comp. Neurol,* 487**,** 147-65.

XU, S. A., MCANALLY, K. I., XU, J. & CLARK, G. M. 1993. Comparison of half-band and full-band electrodes for intracochlear electrical stimulation. *The Annals of otology, rhinology, and laryngology,* 102**,** 363-7.

ZHU, Z., TANG, Q., ZENG, F.-G., GUAN, T. & YE, D. 2012. Cochlear-implant spatial selectivity with monopolar, bipolar and tripolar stimulation. *Hearing research,* 283**,** 45-58.